Notes for ARPS/GDST Case 6: 1-2 June 1999 FWS Supercells

	POD	FAR	CSI
0-hr	Undefined	Undefined	Undefined
1-hr	0.000	Undefined	0.000
2-hr	0.000	Undefined	0.000
3-hr	0.000	1.000	0.000
4-hr	0.000	1.000	0.000
5-hr	0.000	1.000	0.000
6-hr	0.163	0.913	0.060

Table 1: ARPS scores for 1-2 June 1999
Composite Reflectivity Threshold: 41 dBZ
Fuzzy Validation Without Phase Shifting

	POD	FAR	CSI
0-hr	Undefined	Undefined	Undefined
1-hr	0.000	Undefined	0.000
2-hr	0.000	Undefined	0.000
3-hr	0.000	1.000	0.000
4-hr	0.028	0.968	0.015
5-hr	0.224	0.848	0.100
6-hr	0.351	0.755	0.169

Table 2: ARPS scores for 1-2 June 1999
Composite Reflectivity Threshold: 41 dBZ
Fuzzy Validation With Phase Shifting

The radius of the verification kernel is 5nm (9.25 km). NIDS non-numeric data is set to 0 dBZ and the composite reflectivity is calculated using only grid points matched with observations

ARPS Initialization at 2100Z 1 June 1999:

- METAR and Oklahoma Mesonet Observations.
- NIDS Reflectivity (AMA, DDC, DYX, FDR, FWS, GLD, ICT, INX, LBB, MAF, SHV, SRX, TLX, TWX, VNX).
- IR Satellite Data.
- Radar Retrievals (SRX, INX).
- 9-km ARPS background field initialized 1800Z 1 June 1999.

Note 1: SOP99 3-km forecast is interpolated to 133x133 3-km verification grid centered on FWS before scores are calculated.

Note 2: Due to the lack of observed convection at the beginning of this forecast, we may want to rerun this case with the model initialized at 0000Z 2 June 2000.

	POD	FAR	CSI
0-hr	1.000	0.000	1.000
1-hr	0.147	0.000	0.147
2-hr	0.092	0.000	0.092
3-hr	0.000	1.000	0.000
4-hr	0.028	0.968	0.015
5-hr	0.224	0.848	0.100
6-hr	0.351	0.755	0.169

Table 3: GDST scores for 1-2 June 1999
Composite Reflectivity Threshold: 41 dBZ

	POD	FAR	CSI
0-hr	1.000	0.00	1.00
1-hr	0.211	0.600	0.160
2-hr	0.000	1.000	0.000
3-hr	0.000	1.000	0.000
4-hr	0.000	1.000	0.000
5-hr	0.000	1.000	0.000
6-hr	0.000	1.000	0.000

Table 4: Persistence forecast scores for 1-2 June 1999
Composite Reflectivity Threshold: 41 dBZ

Case 6: Summary

A severe weather event in northern Texas on 1-2 June 1999 propagated through the Forth Worth area. Because NIDS data is void of convective activity at 21Z, June 1, 1999, the GDST is initialized at 22Z as a line of convection develops northwest of the KFWS radar (Figure 2). The GDST produces an accurate representation of the large-scale motion of the convective line as it propagates eastward. However, at 22Z the convective line is still in its formative stage. Therefore, as the line continues to grow in areal coverage and intensity past 22Z, the GDST forecast cannot accurately portray the convective evolution.

This explains the POD of 0.147 at hour 1 decreasing to a POD of 0.0 at hour 3. The false alarm rates remains 0.0 through hour 2 since the GDST forecast correctly forecasts the eastward propagation of one particular storm within the convective line. But the POD values also remain low because the areal extent of convection with composite reflectivity above 41 dBZ is much greater than actually forecast.

An ARPS 3-km, 0- to 6-hr real-time forecast generated over the Southern Plains captures this event. Considering the forecast results first in a subjective sense, the ARPS forecast showed some level of usefulness:

1. *Storm Complex Structure*. The model initiates and maintains a broken line of isolated and intense convective cells.

2. *Orientation*. The forecast storms are orientated along a northeast-southwest line through most of the verification domain, in good agreement with the observed storms.

However, there are four major errors present with this forecast which overshadow the successes listed above. The error types are:

1. *Time Lag*. The model generates storms over two hours after convection is indicated on radar, resulting in zero skill (according to the statistics) at 1- and 2-hours. The model is also slow in decaying the storms at the 6-hour mark, although this issue is not apparent in the statistics.

2. *Phase Error*. The ARPS convection develops along a line that is further east of the observed storms, resulting in zero skill (according to the statistics) at 3- to 5-hours. This error is filtered somewhat by the phase-shifting scheme, resulting in improved statistics at the 4- and 5-hour marks.

3. *Areal Coverage*. The overall coverage of the model significant reflectivity is greater than what is observed from the NIDS data at the 6-hour mark. This is in part related to the time lag mentioned above.

4. *Intensity*. The overall reflectivity of the storms seems to be slightly greater than the observed reflectivity towards the end of the forecast. This error is not apparent in the statistics.

As a result of the time lag and phase errors, the raw statistics generated for this case actually show zero skill up to 5-hours, with the scores improving slightly in the final hour. Filtering out the phase error results in somewhat improved scores from 4- to 6-hours, indicating that the forecast does have a level of skill associated primarily with correctly forecasting the storm type and orientation.

This case points out the potential need for adjusting the size of the kernel used within the fuzzy verification technique. This is based on the premise that larger phase errors can be allowed within longer range (in a temporal sense) forecasts. At later forecast hours, such as within a 6-hour forecast, the exact timing and location of convective activity becomes less important since a forecaster may only want to know if any potential exists for convective activity within the surrounding region relative to the airport terminal.

Therefore, a modification to the radius of tolerance in the fuzzy validation scheme can be made so that it's distance increases with time. For the following statistics in Table 5, the radius is set using the following equation:

$$R = R_0 T$$

where R_0 equals 5 nautical miles (nm) per hour, and T is the forecast time in hours. Using this function, the tolerance radius varies from 0 nm for the forecast initialization to 30 nm (55.5 km) for the 6-hour forecast. With the increased kernel size at later forecast hours, the POD, FAR, and CSI scores are much improved over those in Table 1 for forecast hours 3-6.

	POD	FAR	CSI
0-hr	Undefined	Undefined	Undefined
1-hr	0.000	Undefined	0.000
2-hr	0.000	Undefined	0.000
3-hr	0.012	0.976	0.008
4-hr	0.391	0.640	0.231
5-hr	0.760	0.566	0.382
6-hr	0.843	0.502	0.456

Table 5: ARPS scores for 1-2 June 1999
Composite Reflectivity Threshold: 41 dBZ
Fuzzy Validation Without Phase Shifting
Radius: $R_0 T$
NIDS non-numeric data set to 0 dBZ
Composite Reflectivity Calculated Using Only Grid Points Matched With Observations

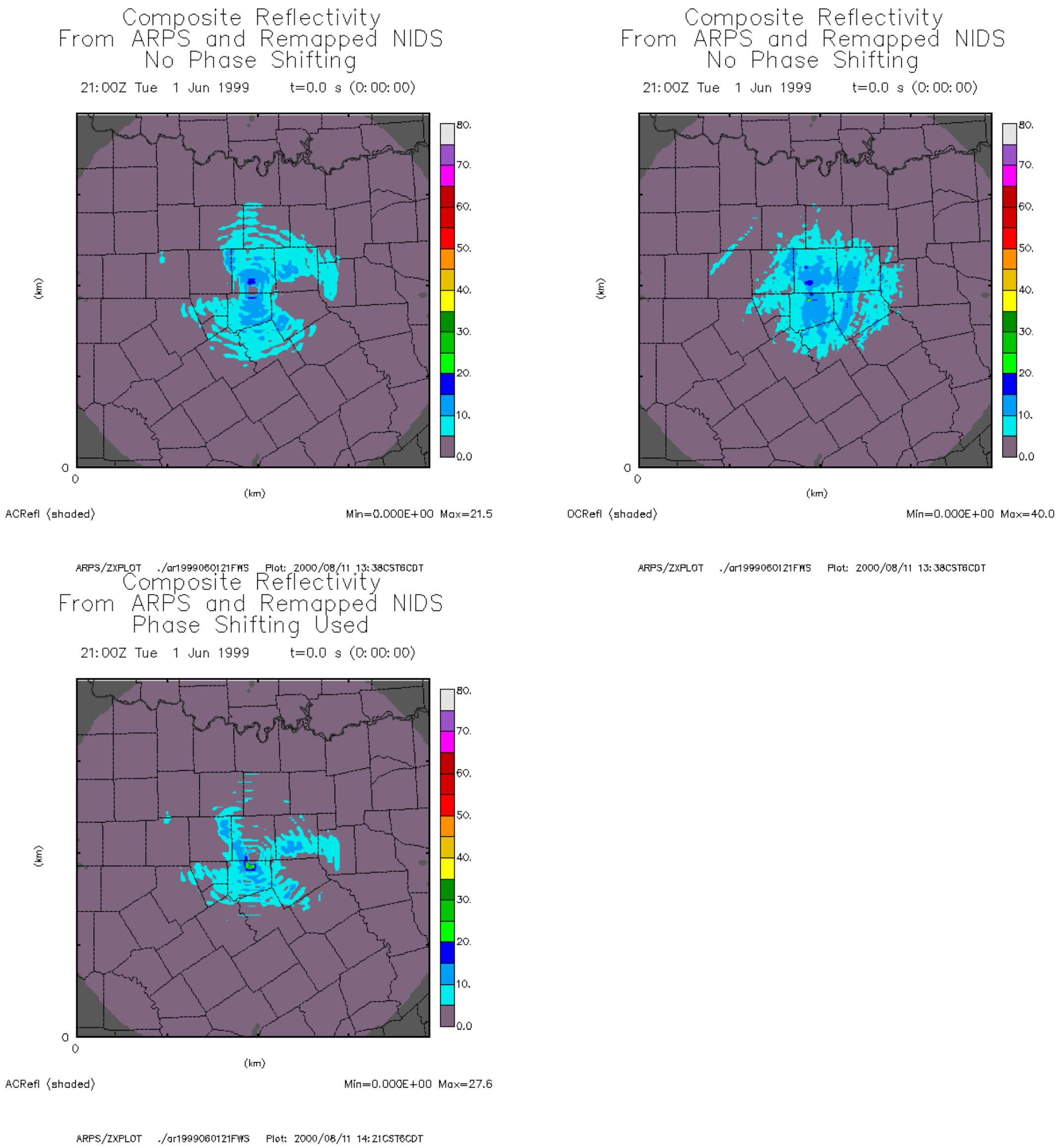

Figure 1: ARPS composite reflectivity forecast initialized at 2100Z 1 June 1999 (upper-left), NIDS composite reflectivity (upper-right), ARPS phase-shifted forecast (lower-left), and the GDST forecast (lower-right). All panels valid for 2100Z 1 June 1999.

Comments: There are no convective cells in the region at the initialization time. All of the scores for this hour are undefined. Because no convective cells exist, the GDST forecast is not begun until 22Z (Figure 2).

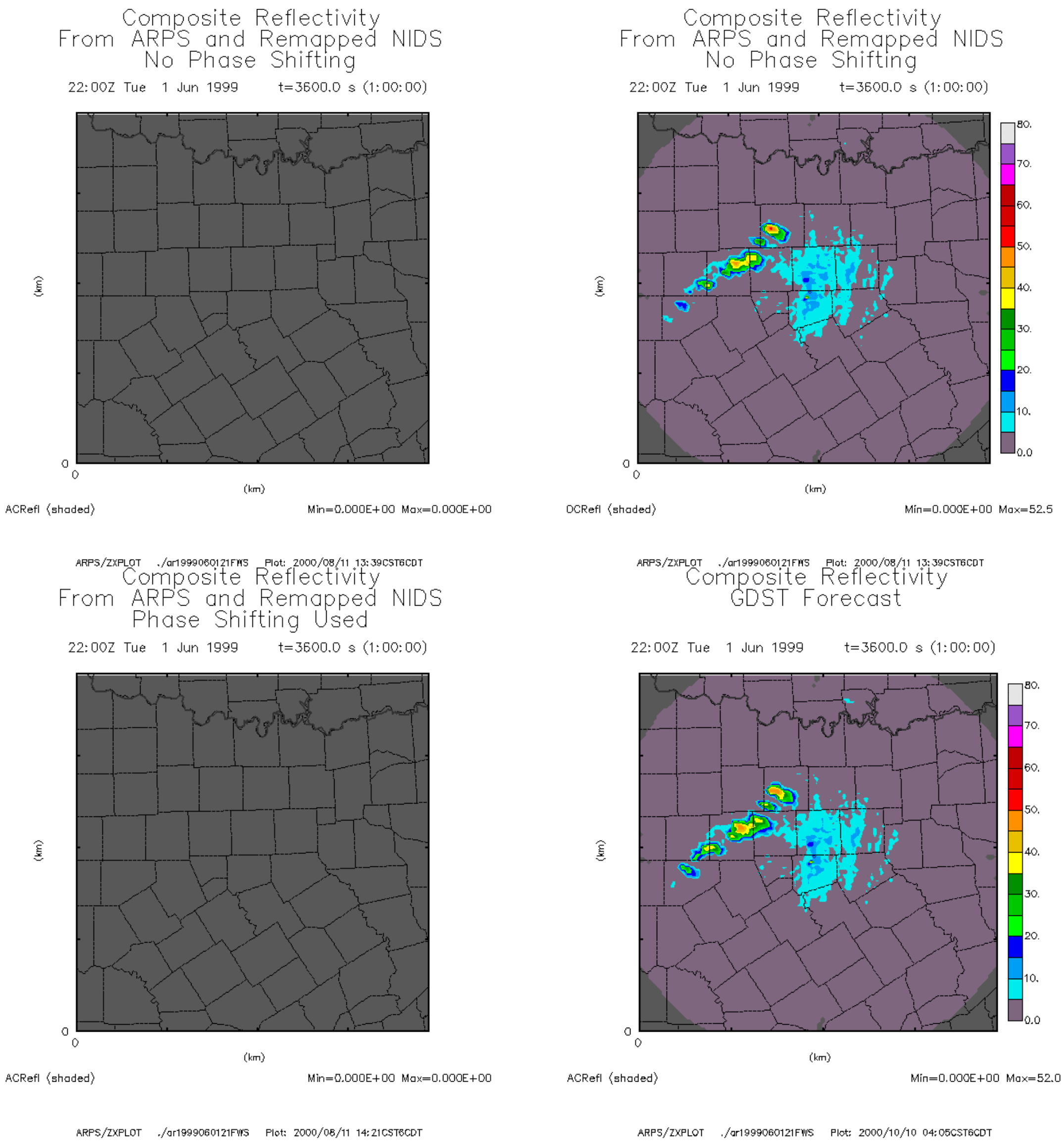

Figure 2: As in Figure 1, but valid 2200Z 1 June 1999.

Comments: A time lag between the ARPS forecast and observations becomes apparent at this hour, as convection begins to develop west and northwest of FWS in the real atmosphere. The model has no reflectivity at this time. 22Z is the initial 0-hour forecast for the GDST since this is the first hour that NIDS data contains convective activity.

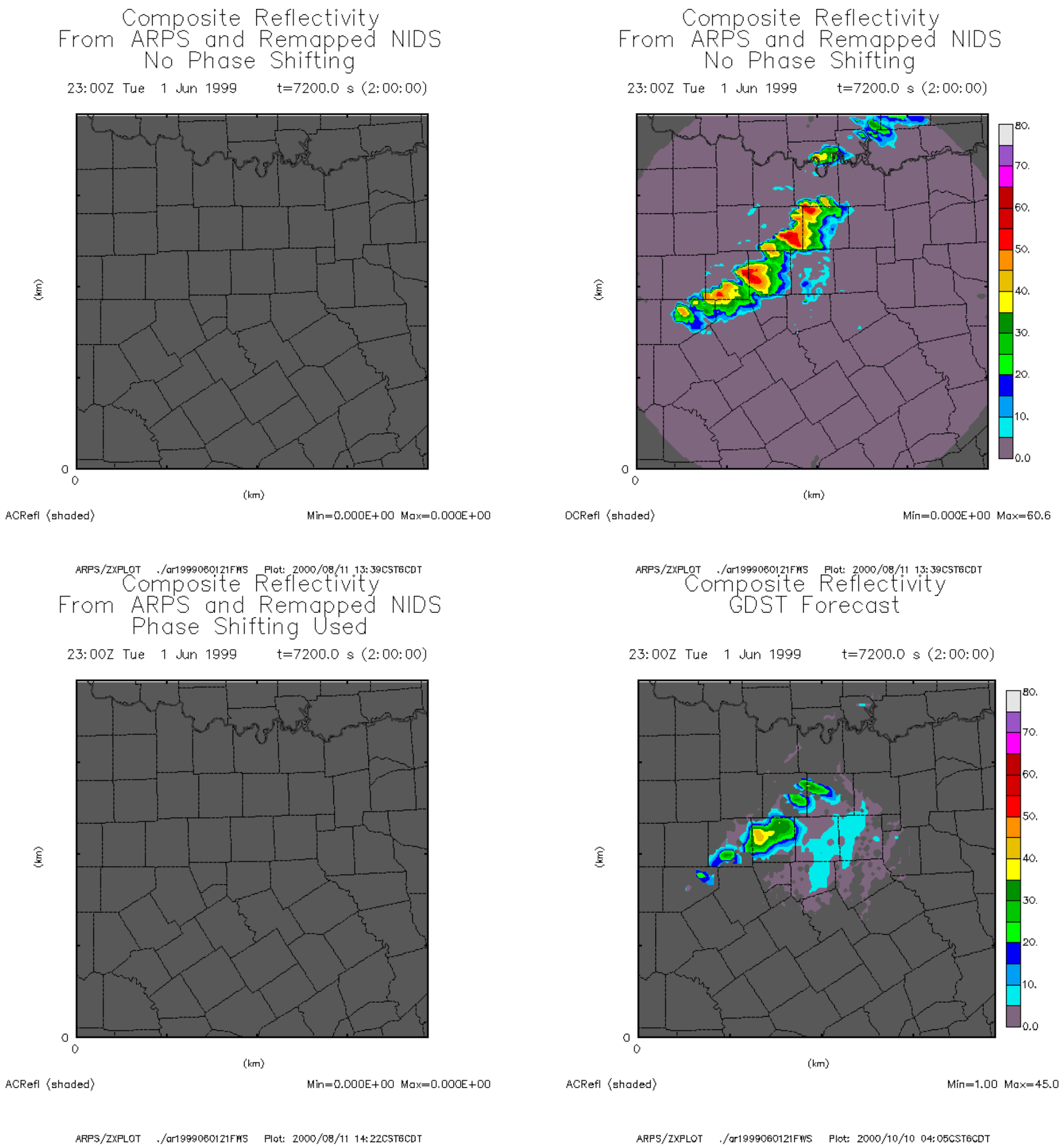

Figure 3: As in Figure 1, but valid 2300Z 1 June 1999.

Comments: The time lag worsens for the ARPS forecast by the two hour mark, as a broken line of supercells with significant reflectivity is observed west to north of FWS. The ARPS model continues to have no reflectivity. GDST correctly propagates the convective line eastward but the new cell development is not captured in the forecast.

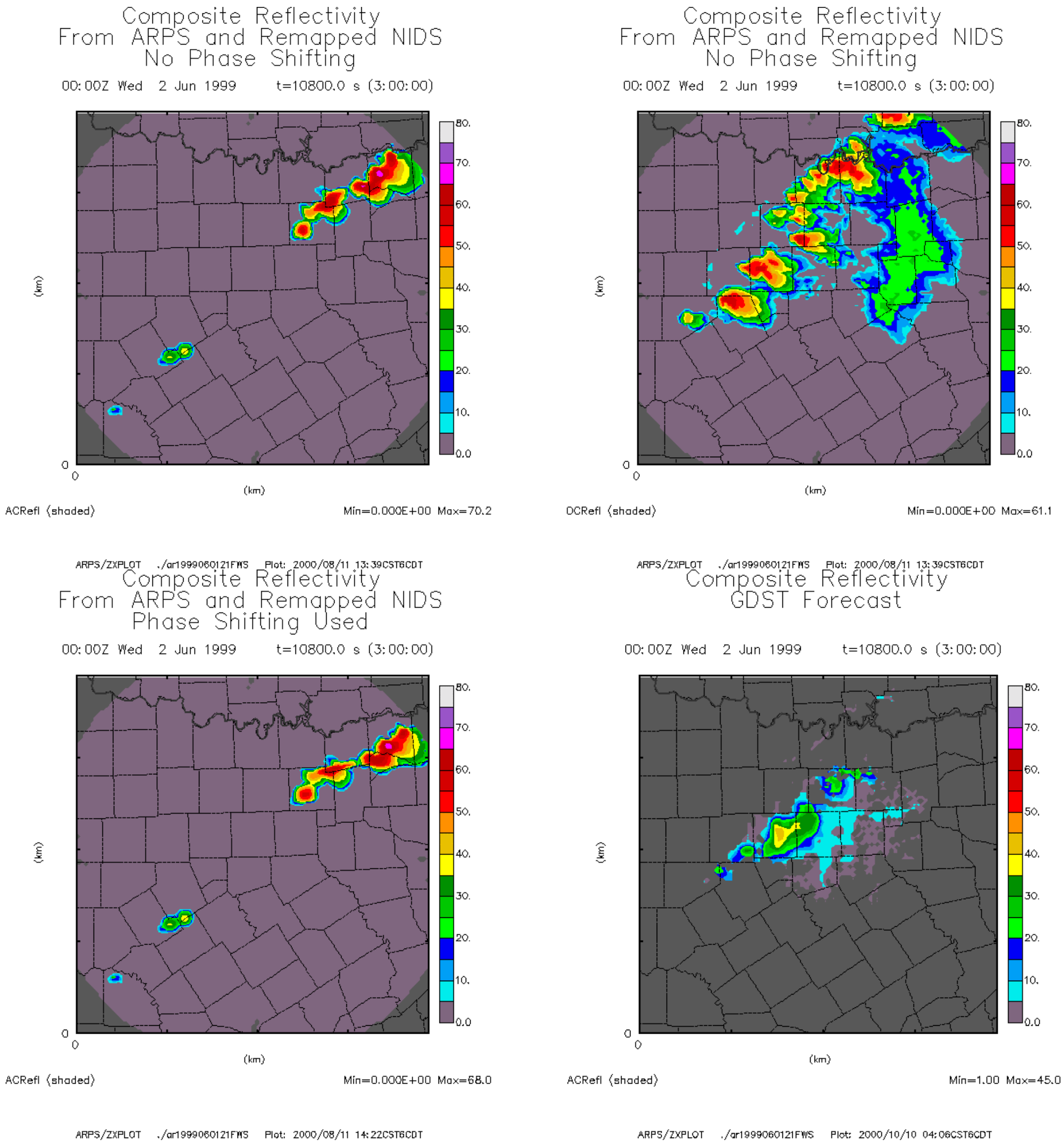

Figure 4: As in Figure 1, but valid 0000Z 2 June 1999.

Comments: At this time the ARPS finally generates storms. Although the northeast-southwest orientation of the model convection matches that of the observed supercells, the forecast storms are too far to the east. Also, the most intense ARPS convection is concentrated along the Red River (including a region where light reflectivity is observed ahead of the supercells), while the NIDS data shows high reflectivity values all along the line of storms. The temporal and magnitude errors probably explain why phase-shifting the forecast fails to improve the statistics. The GDST forecast continues to propagate the convection eastward correctly although again the areal extent is greatly underdone.

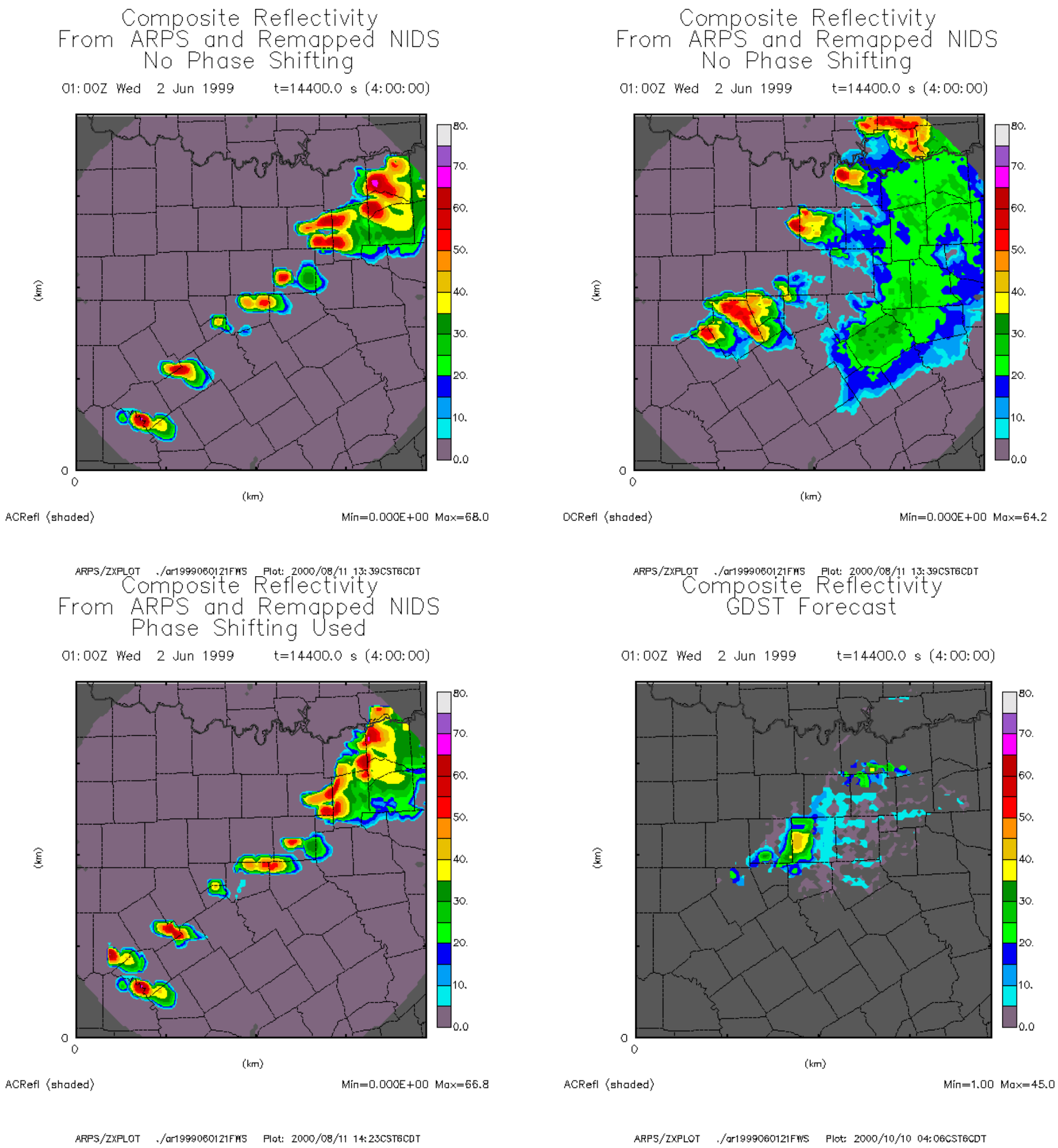

Figure 5: As in Figure 1, but valid 0100Z 2 June 1999.

Comments: By the fourth hour of the forecast, the ARPS model is finally producing intense convective cells all along the line. Unfortunately a number of problems are present: (1) The southwest end of the model convection is further south and west than the observed storms. (2) The ARPS has intense reflectivity in the northeast corner of the verification grid, while the NIDS data has low values (possibly from mid-level convection or anvils?). These problems, along with the fact that both the observed and forecast storms are isolated in nature, prevent the phase-shifting from dramatically improving the forecast. The GDST forecast no longer contains any skill.

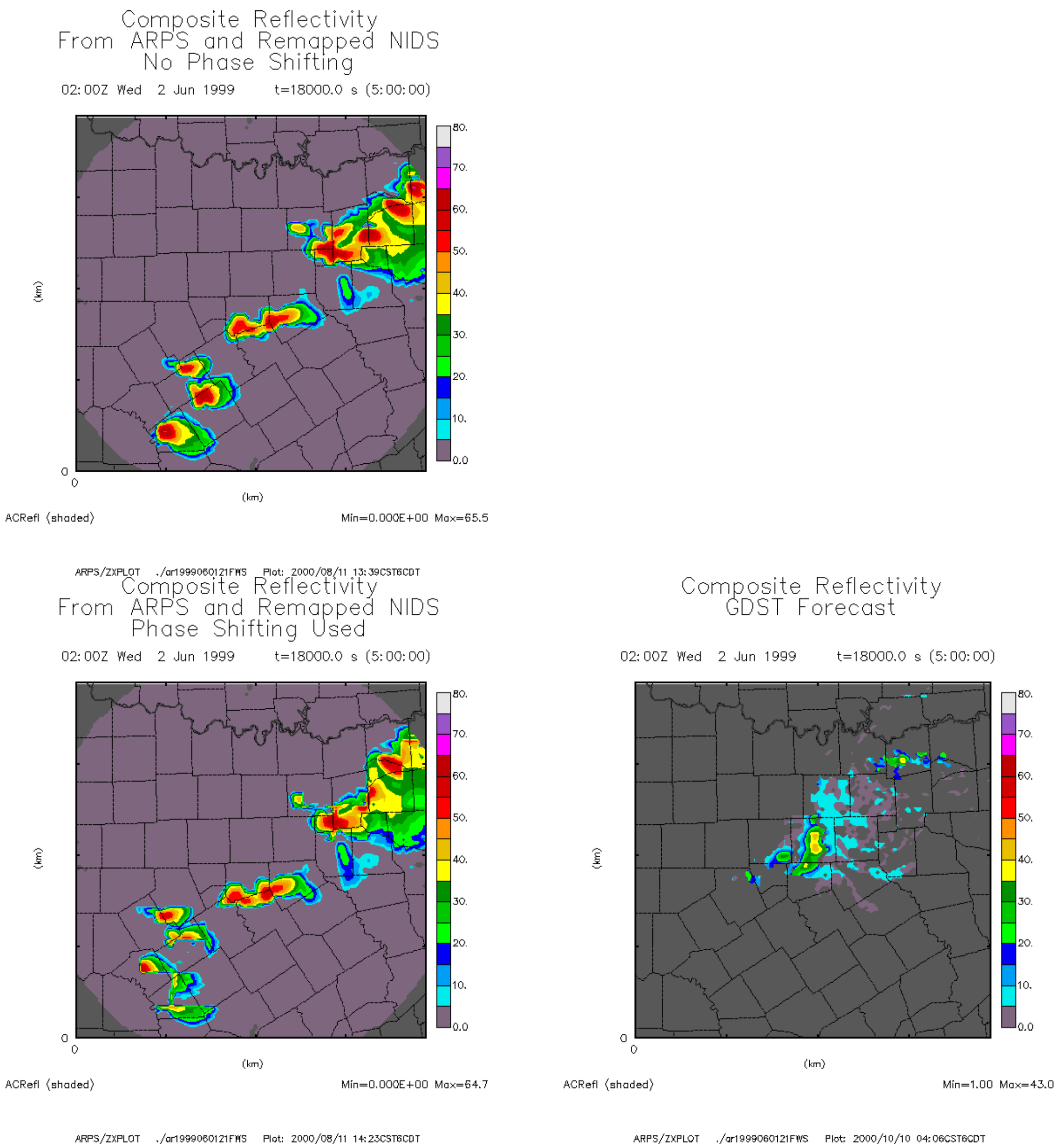

Figure 6: As in Figure 1, but valid 0200Z 2 June 1999. (NIDS composite reflectivity image unavailable.)

Comments: We are unable to plot the NIDS data for this hour, but based on the 0100Z and 0300Z plots it appears that the real storms were dissipating at this time. In contrast, the ARPS still has a long, broken line of storms extending across most of the verification grid. Phase-shifting the forecast improves the statistics somewhat (probably due to observed convection west-southwest of FWS), but the overall performance of the forecast remains poor.

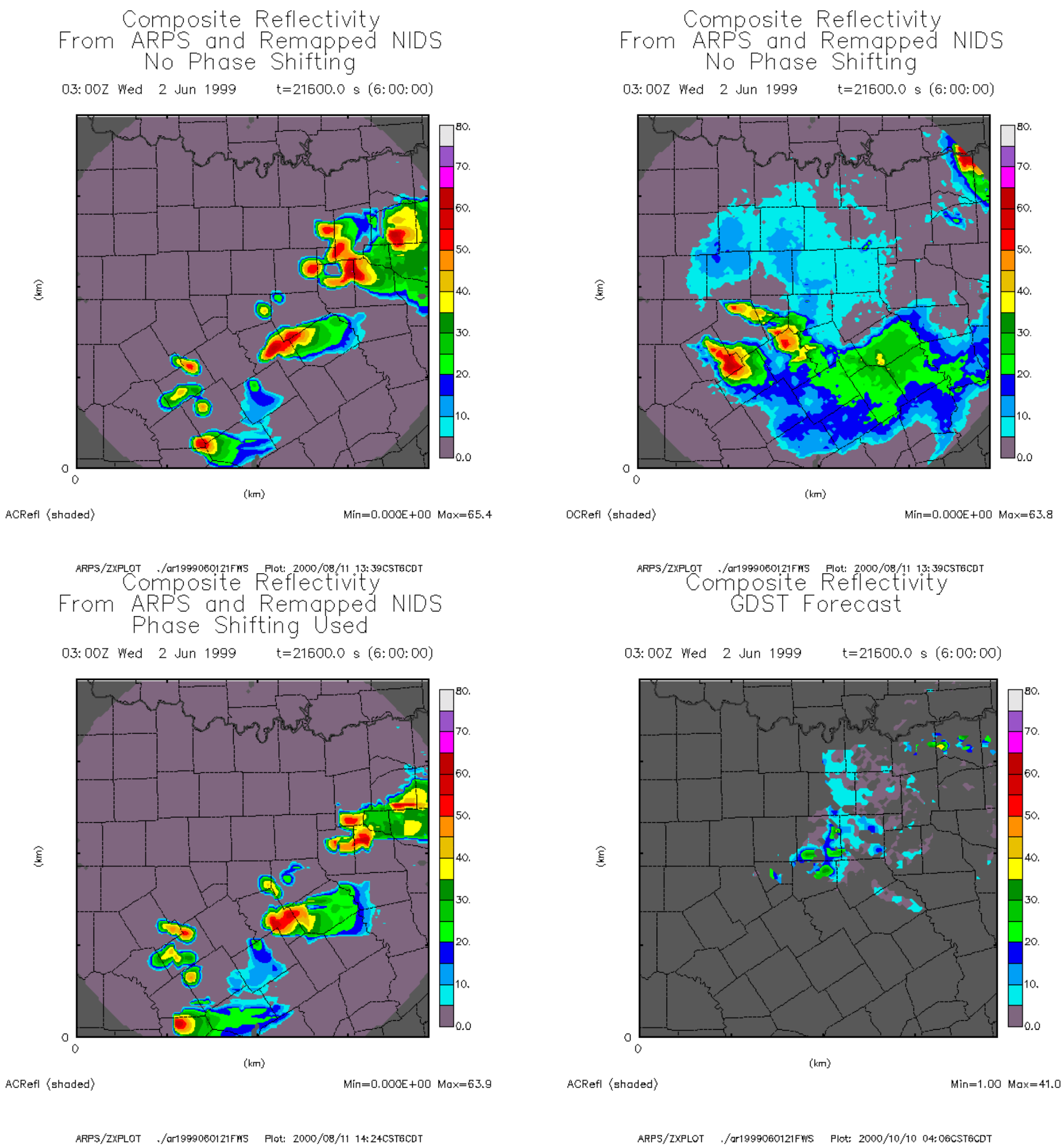

Figure 7: As in Figure 1, but valid 0300Z 2 June 1999.

Comments: In the final hour of the forecast, the model continues to have intense convection in regions devoid of significant NIDS reflectivity. Phase shifting again improves the statistics due to the convection observed southwest of FWS, but the other problems remain with the simulation.